DCC Confers Susceptibility to Depression-like Behaviors in Humans and Mice and Is Regulated by miR-218

Supplemental Information

Supplemental Methods and Materials

Animals

Experimental procedures were performed in accordance with the guidelines of the Canadian Council of Animal Care, and approved by the McGill University and Douglas Hospital Animal Care Committee. All mice used in these studies were maintained in the colony room of the Neurophenotyping center of the Douglas Mental Health University Institute on a 12h light-dark cycle (light on at 8:00h) with ad libitum access to food and water thought out the experiments. Only male mice were included in this study and they were assigned randomly to each experimental condition.

C57BL/6 mice: Adult male C57BL/6 wild-type mice (PD 75±15) obtained from Charles River Canada served as experimental subjects in the chronic social defeat stress paradigm (CSDS). Mice were housed in groups of 4 animals per cage prior exposure to CSDS and singled housed after CSDS.

CD-1 mice: Male CD-1 retired breeder mice (<4 months of age) obtained from Charles River Canada were used as aggressors in the CSDS paradigm. CD-1 mice were used for a maximum 3 consecutive experiments and for no longer than 3 months. CD-1 mice were singled house throughout the study.

Dcc floxed mice: $Dcc^{lox/lox}$ mice (PD 75±15) were originally obtained from Dr. Berns (University of Amsterdam) (1) and are bred at Neurophenotyping center of the Douglas Mental Health University Institute. A transgenic insertion of LoxP sites into the intronic sequences surrounding exon 23 of the *Dcc* gene (Bln1 site (142370-75) and Csp451 site (147663-67)) was achieved by using a targeting vector in the 129S6-derived embryonic stem cell line. This line was backcrossed onto C57BL/6 background for a minimum of 6 generations. Exon 23 is 163 nucleotides in length and encodes the DCC amino acid sequence spanning a portion of the extracellular and transmembrane domains (1077-1130aa). The deletion of exon 23 produces a

frameshift mutation with a number of new putative premature stop codons. Confirmation of the Lox-sites was achieved by PCR as described previously (2). A total of 48 *Dcc*$^{lox/lox}$ were included in this study.

Chronic Social Defeat Stress Paradigm

The CSDS apparatus consisted of a transparent rat cage with two mouse housing compartments separated by a transparent and perforated central divider that allowed sensory but not physical contact between mice. Each selected CD-1 mouse previously screened for aggressive behavior was housed on one of the compartments for at least 24hr before the beginning of CSDS. The other compartment remained empty. The CSDS protocol was the same as in (3,4) and consisted of 10 daily sessions in which an adult wild-type C57BL/6 experimental mouse was introduced into the CD-1 compartment for a period of 5 minutes. At the completion of the session, the C57BL/6 experimental mouse was housed overnight on the empty compartment to provide psychological stress. The procedure was repeated for a total of 10 consecutive days, in which C57BL/6 experimental mice had to be exposed to a new aggressor every day. Control C57BL/6 mice were housed in similar 2-compartment rat cages with a different littermate every day. The CSDS protocol was conducted during the light cycle, between 14:00 and 17:00.

Social interaction test: Twenty-four hours after the last session of CSDS, C57BL/6 experimental mice were assessed in the social interaction test to measure their approach and/or avoidance behavior towards a social target as before (4). Briefly, the social interaction test consisted of 2 sessions in which defeated and control mice were allowed to explore a squared-arena (42cm x 42cm) for a period of 2.5 minutes each session. In the first session, an empty wire mesh enclosure was located against one of the walls of the arena to determine baseline exploration. In the second session, an unfamiliar CD-1 aggressor was placed inside the wire mesh enclosure. The area that surrounded the enclosure was designated as the social interaction zone (14cm x 9cm), and the corners of the wall opposite to the enclosure were designated as corners (9cm x 9cm) and represented the farthest point from the social interaction zone. The time spent (in seconds) in the interaction zone and the corners and the distance traveled (in meters) were estimated during both sessions of the test. The social interaction ratio was calculated as the time spent in the interaction zone with the CD-1 aggressor present divided by the time spent in the interaction zone with the CD-1 aggressor absent. Defeated mice with a ratio<1 were classified as susceptible and a ratio≥1 were classified as resilient (3). All social interaction testing was performed under red-light conditions between 11:00am and 4:00pm and mice were tested in a random order. Animal behavior was recorded with an overhead video camera for offline analysis

using the software TopScanTM 2.0 (Clever Systems Inc., Reston, VA, USA). The mRNA, microRNA, and protein data were derived from tissue samples of susceptible (n=27), resilient (n=27) and control (n=26) mice collected from 3 different and independent CSDS experiments.

Behavioral Tests

Sucrose preference: Mice were habituated to drink water from two 50 ml falcon tubes with sipper tops for 2 consecutive days. On the third day, mice were given a free choice between two bottles containing either 1% sucrose in water or regular tap water. The consumed volume of each solution was measured daily during 4 consecutive days and the position of the bottles was interchanged after each daily measurement. Sucrose preference was estimated by dividing the volume of consumed sucrose by the volume of consumed sucrose + consumed tap water. The average of sucrose preference of the 4 test days was calculated to estimate the total preference for sucrose. Mice that did not habituate to drink from the water bottle were not included in this study.

Elevated plus maze: Anxiety-like behavior was assessed in a plus maze elevated 50 cm from the floor. The maze consisted of two facing open arms and two facing enclosed arms that extend from a central platform. Mice were placed in the center platform of the maze facing one of the open arms and left to explore the arms during five minutes. The time spent in the open versus closed arms of the maze were recorded with an overhead video camera for offline analysis using the software TopScanTM 2.0 (Clever Systems Inc., Reston, VA, USA).

Fear conditioning task: Fear conditioning was adapted from (5) consisted of one training session and a test session completed over two consecutive days. The training took place in an operant chamber (length: 22cm x width: 18.5cm x height: 13cm) with a metal grid floor connected to an electrical current supplier and transparent Plexiglas wall panels. Mouse behavior was recorded using a web camera located in the roof of the operant chamber. The training protocol consisted of two consecutive 80 dB tones (30sec) that ended with a 0.5 mA foot-shock (2sec) delivered through the metal grid floor separated by a 2min inter-trial interval, in which no tone or shock were presented. Once training was complete, mice were immediately returned to their home cage and the operant chamber was cleaned thoroughly with Peroxygard (Bayern, ON, Canada).

The test session consisted of (A) contextual and (B) cued tests. The contextual test consisted of placing the mice in the exact same operant chamber for 4min, but no tone or shock were delivered. Freezing behavior was analyzed during the contextual test. After a 3hours period, the cued test was performed. During this cue test, the animals were placed in different operant

chambers that were substantially different to the ones originally used for the training session and the contextual test. The cue test was exactly as the training conditioning, but no foot-shock was delivered.

Antibodies: All the antibodies used in this study and their specificity are described in detail in Table S1.

Tissue Dissection

Mice from the control, susceptible and resilient groups were euthanized by decapitation 24h after the social interaction test. Brains were removed and flash frozen with 2-methylbutane chilled in dry ice. Bilateral punches of the pregenual medial PFC, including cingulate 1 (Cg1), prelimbic (PrL), and infralimbic (IL) subregions, were taken from 1mm coronal sections corresponding to plates 15-18 of the Paxinos & Franklin mouse atlas (6) as previously (7,8). In a separate experiment, we obtained tissue from the ventral tegmental area (VTA), as described previously.

Western Blot

PFC tissue punches were processed for western immunoblot as before (7,9). Briefly, protein samples (25µg) were separated on a 10% SDS-PAGE and transferred to a nitrocellulose membrane which was incubated overnight at 4°C with antibodies against DCC (BD Pharmingen, Mississauga, ON, Canada, (9)) and α-tubulin (Sigma-Aldrich, Oakville, ON, Canada) for loading control (Table S1). Four biological samples were included per experimental condition.

RNA Extraction and Quantitative Real Time PCR for Mouse Tissue

Total RNA and microRNA fraction were isolated from the mouse frozen tissue with the miRNeasy Micro Kit protocol (Qiagen, Toronto, ON, Canada). All RNA samples were determined to have 260/280 and 260/230 values ≥1.8, using the Nanodrop 1000 system (Thermo Scientific, Toronto, ON, Canada) and an RNA integrity number ≥ 8, using TapeStation (Agilent). Reverse transcription for *Dcc* mRNA was performed using iScript (Bio-Rad, Saint-Laurent, QC, Canada). Real time PCR using SYBR green (Quanta Biosciences, Gaithersburg, MD, USA) was carried out with an Applied Biosystems 7900HT RT PCR system. Data for *Dcc* expression were analyzed by comparing C(t) values using the $\Delta\Delta$C(t) method and *Gapdh* was used as reference gene (Table S2). Reverse transcription for miR-218 was performed using miRNA TaqMan probes (Table S2) and expression levels were calculated using the Absolute Quantitation (AQ)

standard curve method. Real time PCR was run in technical triplicates. The small nucleolar RNA (snoRNA) RNU6B used as endogenous control.

Neuroanatomical Experiments With Mouse Brain Tissue

Mice were anesthetized with an overdose of a combination of ketamine 50mg/kg, xylazine 5mg/kg, acepromazine 1mg/kg injected i.p. and perfused transcardially with 0.9% saline, followed by 4% PFA in PBS (pH 7.4). Coronal sections of the pregenual medial PFC (mPFC) were obtained at 35µm using a vibratome. For double-labeled immunofluorescence, endogenous mouse antibodies were blocked using a mouse Ig blocking reagent (Vector Laboratories, Burlingame, CA, USA). Immunostaining was visualized with either Alexa 488-, Alexa Fluor 555- or Alexa Fluor 633-conjugated secondary antibodies raised in donkey (Life technologies, Toronto, ON, Canada).

In Situ Hybridization

Stress-naïve adult C57BL/6 wild-type were euthanized by rapid decapitation. Brains were removed and flash frozen with 2-methylbutane chilled in dry ice. Coronal sections of the pregenual mPFC at 14µm were obtained using a cryostat, were fixed onto superfrost slides with 4% PFA and endogenous peroxidase was inactivated with 0.3% H_2O_2. Slices were then permeabilized with Proteinase K solution and underwent acetylation with triethanolamine and acetic anhydride. Slices were then dehydrated in increasing concentrations of ethanol and permeabilized with Proteinase K solution. Sense and antisense 5' digoxigenin-labeled LNA probes against miR-218 (Table S2) were then hybridized to the slices for 14hr at 60°C. After hybridization, brain sections were stringently washed in saline-sodium citrate (SSC) and 50% formamide for 30 min at 60°C, treated with RNAse A for 30hr at 37°C and washed in decreasing concentrations of SSC. PFC tissue was incubated overnight at 4°C with an anti-DIG antibody coupled to horseradish peroxidase (Roche, Mississauga, ON, Canada) and an anti-DCC antibody #2473 (10). To reveal miRNA expression, sections were incubated with tyramide-coupled to Cy3 (Perkin Elmer, Montréal, QC, Canada) and Alexa 488-coupled secondary antibody raised in goat (Life Technologies, Toronto, ON, Canada) to reveal DCC immunofluorescence. Sections were rinsed in PBS containing Hoechst staining before being coverslipped with Fluoromount-G (SouthernBiotech, Birmingham, AL, USA).

In Silico Analysis and miRNA Identification

Candidate miRNAs to regulate DCC expression were predicted using five miRNA target prediction databases: miRWalk (11), miRanda (12), miRDB (13), Diana-microT (14), and TargetScan (15). Only miRNAs that were predicted by at least three out of the five databases and were confirmed to be expressed in human and mouse brain were selected for downstream experiments. miRNAs were ranked according to their mirSVR predicting score, which is a prediction system that determines the potential of a miRNA to regulate the expression of specific target genes (16), and selected the miRNA with the highest mirSVR score.

Human Brain Samples

Ethics approval was obtained from the research ethics board at the Douglas Mental Health University Institute. Postmortem prefrontal cortex (Brodmann area 44; BA44) tissue samples were obtained in collaboration with the Quebec Coroner's Office and the Douglas-Bell Canada Brain Bank (Douglas Mental Health University Institute). Written informed consent was obtained from the family of each deceased subject before inclusion in the study. Psychological autopsies were performed based on Diagnostic and Statistical Manual of Mental Disorders (DSM)-IV criteria. Control subjects had no history of suicidal behavior, major psychiatric disorders or antidepressant treatment.

Subjects

Validation cohort – This cohort consisted of 11 depressed subjects who committed suicide and 12 sudden-death controls. All depressed subjects were antidepressant-free for at least 3 months prior to death by suicide. A subset of this group had history of substance abuse (n=4). There were no differences between groups in age, brain pH, RNA integrity number and postmortem intervals.

Original cohort – This cohort consisted of 24 depressed subjects who committed suicide and 35 sudden-death controls. The depressed group included subjects with comorbid MDD and substance abuse (n=2) to match the diagnostic characteristics of the validation cohort. There were no differences between groups in age, brain pH, RNA integrity number and postmortem intervals.

RNA isolation and quantitative Real time-PCR for human tissue: Total RNA (including miRNA fraction) was isolated from human postmortem frozen brain tissue as we reported previously (4).

Total mRNA was reverse transcribed using M-MLV reverse transcriptase and oligo(dT)16 primers. miRNA was reverse transcribed using TaqMan RT-PCR microRNA assays (Table S2; Applied Biosystems, Toronto, ON, Canada) according to the manufacturer's instructions. Real-time PCR reactions were run in technical quadruplets using the ABI 7900HT Fast Real-Time PCR System (Applied Biosystems, Toronto, ON, Canada). TaqMan probes were used to measure mRNA and miRNA expression. Expression levels were calculated using the Absolute Quantitation (AQ) standard curve method, with *GAPDH* used as the reference gene for mRNA quantification and RNU6B for miRNA. The qPCR efficiencies range between 90% and 110%, with slopes between -3.10 to -3.50. The correlations are between 0.98 and 0.99.

Neuroanatomical Experiment With Human Brain Tissue

Coronal sections (14µm-thick) containing the prefrontal cortex (Brodmann area 44; BA44) and corresponding to plates 09 to 10 of the human brain atlas (17) were treated as described above. Slices were incubated overnight at 4°C with an anti-DIG antibody coupled to alkaline phosphatase (Roche, Mississauga, ON, Canada) and with anti-DCC antibody #2473 (10). Tissue was treated with Fast-Red (Sigma-Aldrich, Oakville, ON, Canada) to label miR-218. The sections were then incubated with a goat anti-rabbit antibody coupled to biotin (Life Technologies, Toronto, ON, Canada), followed by ABC kit incubation (Vector Laboratories, Burlingame, CA, USA). DCC labeling was revealed using 3,3'-Diaminobenzidine substrate (Vector Laboratories, Burlingame, CA, USA) and slides were coverslipped with Fluoromount-G (SouthernBiotech, Birmingham, AL, USA).

Human Neuroblastoma IMR-32 Cell Line

IMR-32 cells were kindly provided by Dr. Lamarche-Vane (McGill University). IMR-32 cells were culture in Dulbecco's modified Eagle's medium (DMEM; Wisent Inc., Saint-Jean-Baptiste, QC, Canada) containing 10% fetal bovine serum (FBS), supplemented with 50 units/ml penicillin and 50µg/ml streptomycin (Invitrogen, Toronto, ON, Canada) in a 5% CO_2 humidified incubator at 37°C. Cell number and viability were determined by trypan blue dye exclusion in a Neubauer hemocytometer. Endogenous expression of miR-218 and DCC was confirmed with quantitative PCR and western blot, respectively.

DCC immunofluorescence: Culture IMR-32 cells were harvested by trypsinization and platted on glass coverslips for 24h. Cells were fixed with 4% PFA and were permeabilized with 0.1% Tween in PBS and blocked with 2% BSA and 2% Goat serum. Incubation against DCC antibody #2473 (10) in blocking solution was performed overnight at 4°C.

Western blot: IMR-32 cells were harvested from DMEM medium and clean with PBS before homogenization. Protein samples (25µg) were processed for western immunoblotting as described above (7).

miRNA Mimic Transfection Experiment

A total of 4 x 10^5 IMR-32 cells were grown in the continuous presence of either HiPerfect transfection reagent alone (Mock), a miR-218 mimic (5nM), or a miR-mimic scramble (5nM) control for 24h, according to the manufacturer's protocol (Qiagen, Toronto, ON, Canada). A mimic is a synthetic double-stranded miRNA that comprises the same function as endogenous miRNAs (18).

Target Protector Experiment

A total of 4 x 10^5 cells were grown for 24h with HiPerfect transfection reagent alone, or transfection reagent in combination of the miR-218 mimic and two target protectors, according to the manufacturer's protocol (Qiagen, Toronto, ON, Canada). A target protector is an oligonucleotide designed to prevent miRNAs from binding specific mRNA targets (28). The sequences of the two target protectors included nucleotides 66 to 73 (target protector 1) and nucleotides 513 to 518 (target protector 2) of the 3'UTR of the *DCC* mRNA. These two sequences correspond to the specific binding sites between miR-218 and *DCC* 3'UTR. The mimic and target protector experiments were performed in biological triplicates. Confluent cultures were harvested by trypsinization (0.125 trypsin/1% EDTA in PBS) and homogenized using the miRNeasy Mini Kit (Qiagen, Toronto, ON, Canada). The expression of *DCC*, *ROBO1* and miR-218 were assessed with real time PCR as described for the human and mouse experiments and samples were run in technical triplicates.

Stereotaxic Surgery

Adult *Dcc*$^{lox/lox}$ mice were deeply anesthetized with Isoflurane (5% for induction and 2% for maintenance) and placed in a stereotaxic apparatus. Adeno-Associated Virus (AAV8) expressing a Cre-GFP fusion protein under the control of the calcium calmodulin kinase II alpha (CaMKIIα) promoter (AAV8-CaMKIIα-CreGFP) or control virus (AAV8-CaMKIIα-GFP) were infused bilaterally into the prelimbic/infralimbic subregion of the medial PFC at the following coordinates: +2mm (A/P), ±0.5mm (M/L), and -2.7 (D/V) relative to Bregma. Viral constructs were obtained from University of North Carolina (UNC Vector Core, Chapel Hill, NC, USA). A total volume of 0.5 µl of virus was delivered on each hemisphere over a 6min period. The infusion cannula was

left inside the brain area during a 6min pause to avoid virus reuptake. Mice were allowed to recover for 21 days before behavioral experiments. At the completion of the behavioral testing, experimental mice were perfused as described above and coronal sections were examined to confirm robust viral expression at the site of injection.

Stereology

Stereological counts of SMI-32-positive pyramidal neurons in the pregenual mPFC were performed in a subset of *Dcc*$^{lox/lox}$ mice infected with AAV8-CaMKIIα-GFP (n=5) or with AAV8-CaMKIIα-CreGFP (n=5) as previously (2). Briefly, the total number of SMI-32-positive neurons at the site of injection between PrL and IL subregions of the mPFC was evaluated using a stereological fractionator sampling design, with the optical fractionator probe of the Stereo Investigator® software (MicroBrightField, Williston, VT, USA). Regions of interest were delineated according to 5× magnification using a Leica DM4000B microscope (Leica, Concord, ON, Canada). Sections spanning plates 14–18 of the Paxinos & Franklin mouse atlas (6) were analyzed. Counting was performed at 40× magnification in a 1:6 series. A guard zone of 5µm was used. The coefficient of error (CE) was below 0.1 for all brains. Counts were performed blind.

Statistical Analysis

All values were represented as scatterplot with the mean ± s.e.m. Statistical analysis was performed using Graphpad Prism 6.0. A significance threshold of $\alpha < 0.05$ was used in all the experiments. Statistical differences between two groups were analyzed with Student's t-tests. Correlations were calculated using the Pearson correlation coefficient with one-tailed analysis. Otherwise one-way or two-way ANOVAs were performed, followed by Bonferroni's or Tukey's multiple comparison tests. No statistical methods were used to determine the sample sizes, but the number of experimental subjects is similar to sample sizes routinely used in our laboratory and in the field for similar experiments. All data were normally distributed and variance was similar between groups, supporting the use of parametric statistics.

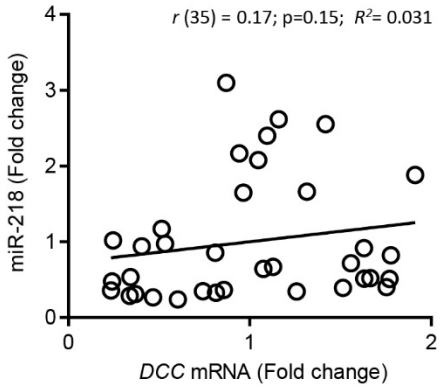

Figure S1. Lack of correlation between *DCC* mRNA and miR-218 expression in the PFC of sudden death control subjects in the original cohort.

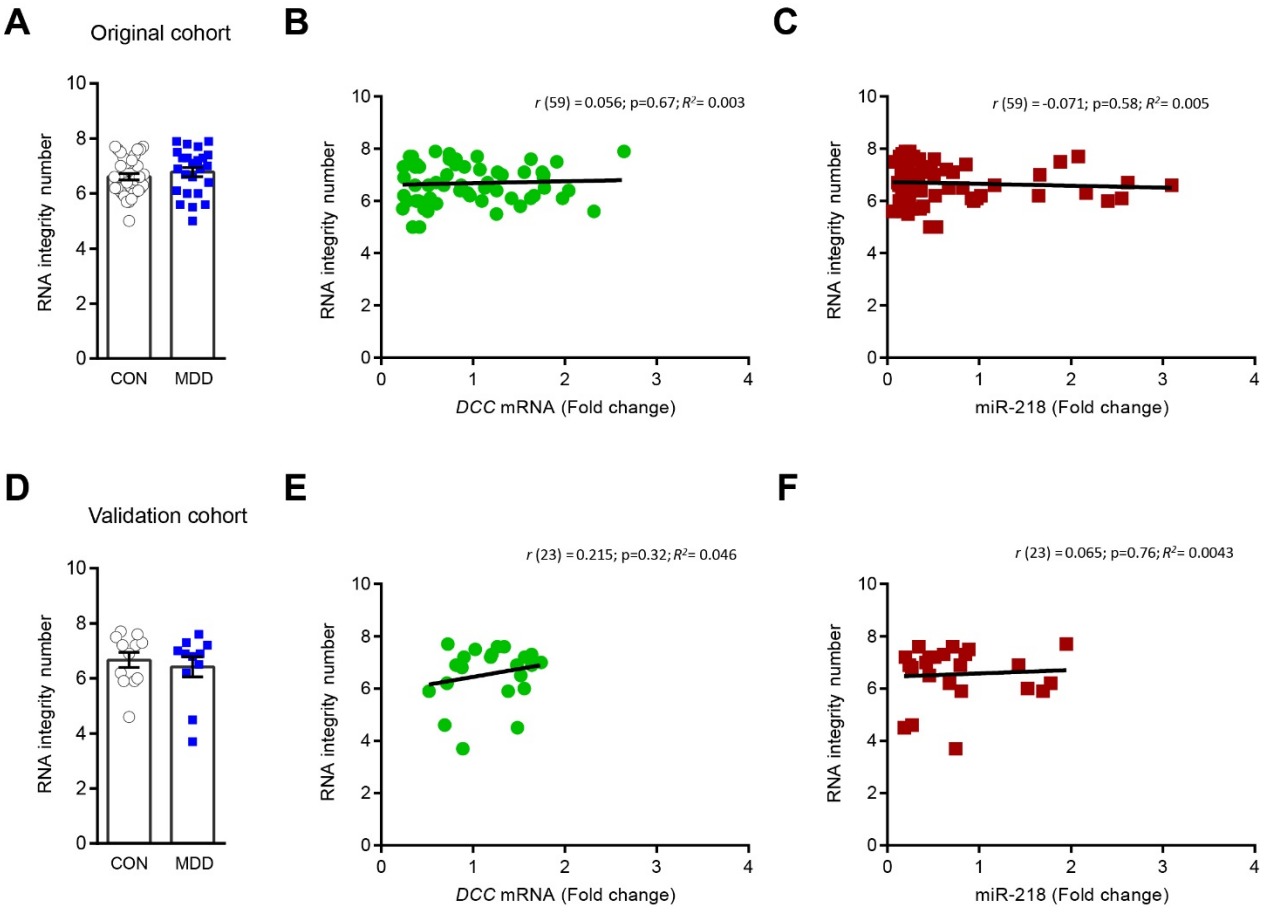

Figure S2. RNA integrity number (RIN) in post-mortem human samples. (A) There are no significant differences in the RIN between control and depressed subjects who died by suicide in the original cohort ($t_{(57)}$=0.84, p=0.4). **(B)** Lack of correlation between RIN versus *DCC* mRNA expression and **(C)** RIN versus miR-218 expression in the PFC of all subjects included in the original cohort. **(D)** There are no significant differences in the RIN between control and depressed subjects who died by suicide in the validation cohort ($t_{(21)}$=0.55, p=0.58). **(E)** Lack of correlation between RIN versus *DCC* mRNA expression and **(F)** RIN versus miR-218 expression in the PFC of all subjects included in the validation cohort.

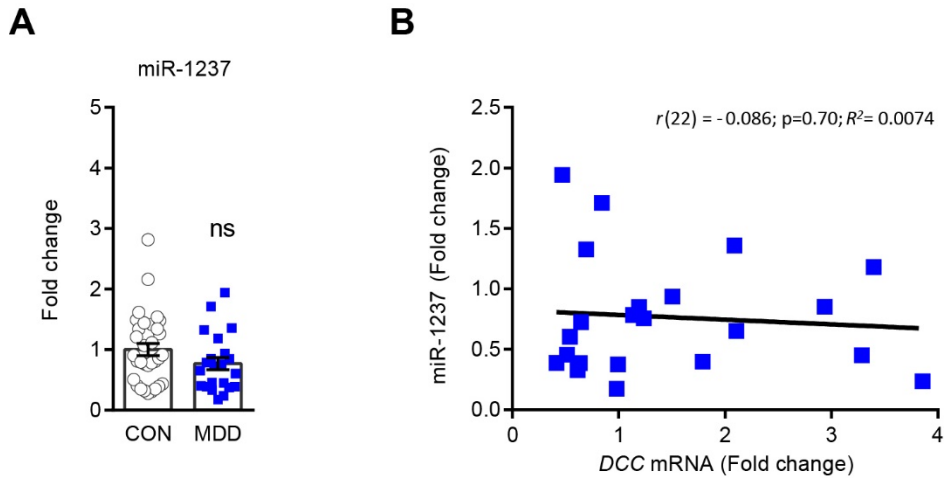

Figure S3. Expression of the primate-specific miRNA, miR-1237, in original cohort. (A) There are no significant differences in the PFC levels of miR-1237 between control and depressed subjects who died by suicide in the original cohort ($t_{(52)}$=1.55, p=0.12). **(B)** Lack of correlation between *DCC* mRNA and miR-1237 expression in the PFC of sudden death control subjects in the original cohort.

Table S1. List of antibodies used for immunofluorescence, western blot and in situ hybridization experiments.

Antigen	Immunogen	Manufacturer	Application	Dilution
DCC	C-terminal peptide (SEESHKPTEDPASV) corresponding to amino acids 1406–1419 of the mouse DCC protein. The specificity of this antibody was demonstrated previously (10).	Dr. Helen M. Cooper, University of Queensland (Cat. #2473), rabbit polyclonal	ICC ISH	1:500 1:1000
SMI-32	Raised against a nonphosphorylated epitope in neurofilament H. Recognizes a subpopulation of pyramidal neurons.	Covance, (Cat. #14941802), monoclonal mouse	ICC	1:1000
Parvalbumin	Raised against Parvalbumin, clone parv-19.	Sigma-Aldrich, (Cat. #P3088), mouse monoclonal	ICC	1:2000
DCC	Truncated recombinant human DCC protein containing the intracellular domain, clone G97-449. This antibody recognizes a major band at ~185 kDa. The specificity of this antibody was previously demonstrated in (9). See Figure S7.	BD Pharmingen, (Cat. #554223), mouse monoclonal	WB	1:1000
Tubulin	Raised in mouse and recognizes an epitope located at the C-terminal end of the α-tubulin isoform. This antibody recognizes a major band at ~50 kDa.	Sigma-Aldrich, (Cat. #T9026), mouse monoclonal	WB	1:4000
α-DIG-POD	Polyclonal antibody specific to digoxigenin and digoxin.	Roche, (Cat. #11207733910), sheep polyclonal	ISH	1:2500
α-DIG AP	Polyclonal antibody specific to digoxigenin and digoxin.	Roche, (Cat. #11093274910), sheep polyclonal	ISH	1:1000

Table S2. List of probes, references and sequences used for real time PCR and in situ hybridization.

Gene Target	TaqMan Assay	SYBR Green	miRCURY LNA Probe
hsa-miR-218	000521		18111-01
U6, hsa/mmu/rno			99002-01
RNU6B	001093		
DCC	Hs00180437_m1		
ROBO 1	Hs00268049_m1		
GAPDH	Hs02758991_g1		
Dcc		Mouse sequence Forward: GTACTCTTCGGAGCTTCCTTG Reverse: TCCATTAGGAAGTTGCTGCT	
Gapdh		Mouse sequence Forward: AGGTCGGTGTGAACGGATTTG Reverse: TGTAGACCATGTAGTTGAGGTCA	

Table S3. List of potential microRNAs (miRNAs) to regulate *DCC*.

Candidate miRNAs predicted by at least 3 databases and expressed in the human and mouse brain were selected. miRNAS were ranked according to their mirSVR predicting score, which is a prediction system that determines the potential of a miRNA to regulate the expression of specific target genes[5]. The starts indicate the miRNAs that fulfilled our criteria.

A total of 13 candidate miRNAs were predicted to bind to the 3'UTR of *DCC* by miRWalk, microRNA.org, and TargetScan. Out of these miRNAs, miR-218 has the highest mirSVR predicting score.

MiRNA, miR-1237, has a high mirSVR score, but it is not expressed in the mouse brain.

miR Name	Database (3)	Human Brain	Mouse Brain	mirSVR
miR-218	*	*	*	**-1.295**
miR-1237	*	*		-1.22
miR-26a-1	*	*	*	-0.6498
miR-486-5p	*	*	*	-0.557
miR-17-3p	*	*	*	-0.3196
miR-19a	*	*	*	-0.1872
miR-19b	*	*	*	-0.1872
miR-15a	*	*	*	-0.1483
miR-15b	*	*	*	-0.1469
miR-195	*	*	*	-0.1455
miR-16	*	*	*	-0.1349
miR-129-5p	*	*	*	-0.1105
miR-25	*	*	*	-0.0731

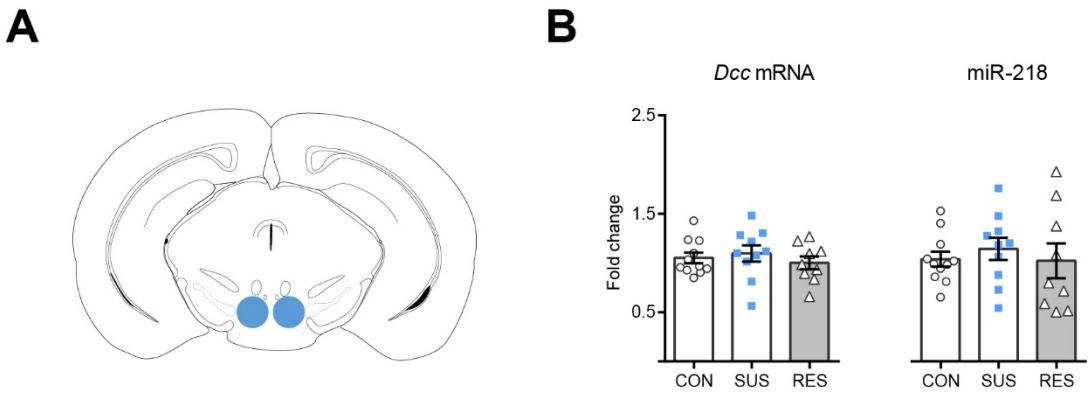

Figure S4. Levels of *Dcc* mRNA and miR-218 in the VTA after CSDS. (A) Schematic of the VTA. **(B)** There are no significant differences in the VTA levels of *Dcc* mRNA and miR-218 between mice exposed to CSDS and stress-naïve controls. *Dcc* mRNA: $F_{(2,27)} = 0.47$; $p = 0.63$. miR-218: $F_{(2,27)} = 0.28$; $p = 0.75$; n = 10-11. CON= Control, SUS= Susceptible, RES= Resilient.

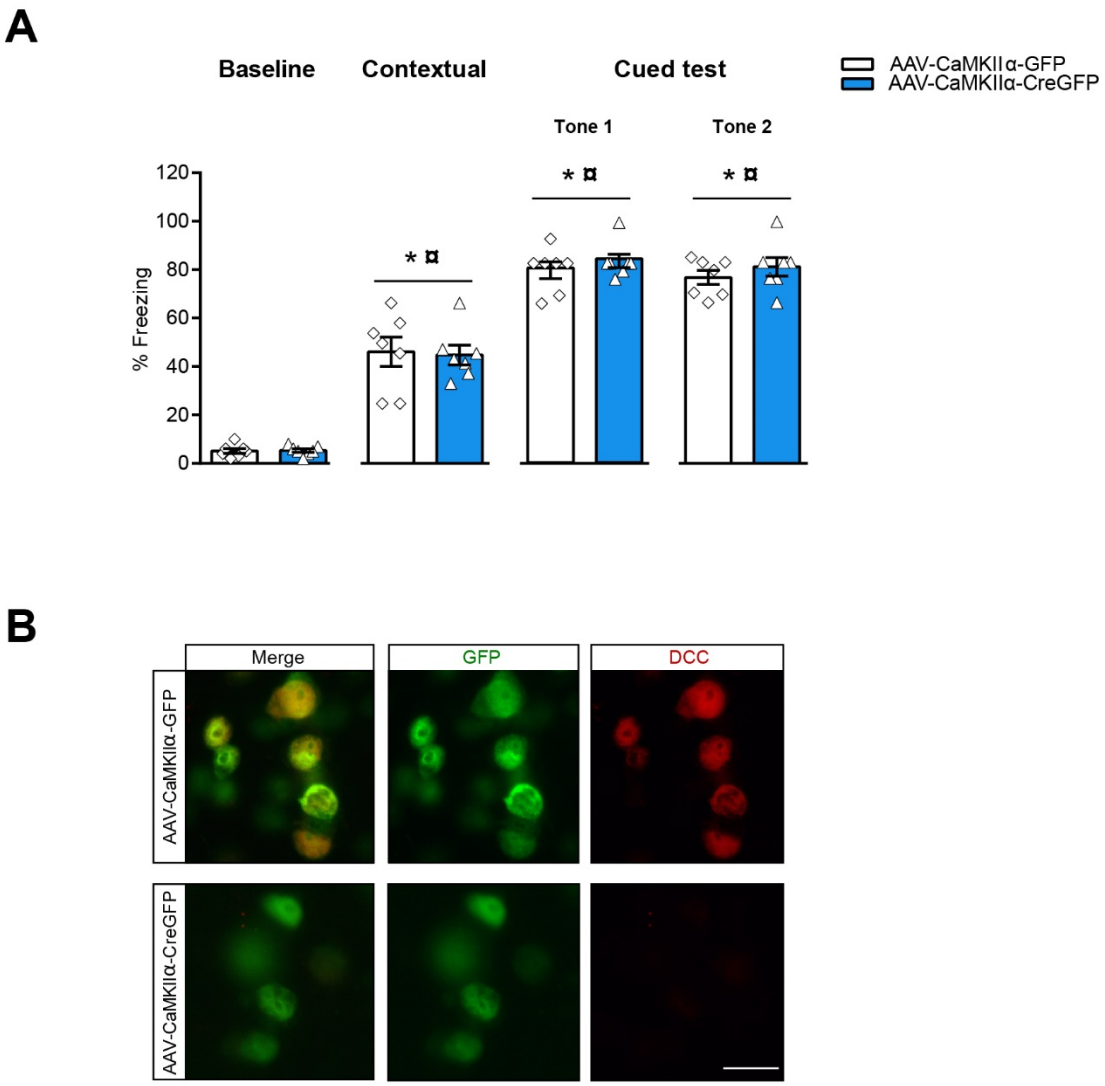

Figure S5. Knocking out *Dcc* in PFC pyramidal neurons does not affect fear conditioning. (A) Contextual and cue-dependent fear conditioning responses are not significantly different in *Dcc*$^{lox/lox}$ mice that received the AAV-CaMKIIα-CreGFP (n=7) versus AAV-CaMKIIα-GFP (n=7) control construct (Two-way ANOVA: session: $F_{(3,48)}$=213; p<0.0001; session by virus interaction: $F_{(3,48)}$=0.31; p=0.81; virus: $F_{(1,48)}$=0.50; p=0.48. Bonferroni's test: *¤p<0.0001. Bonferroni's test: *¤p<0.0001; *Different from baseline control-AAV-CaMKIIα-GFP, ¤Different from baseline control-AAV-CaMKIIα-CreGFP. (B) Validation of *Dcc* deletion in GFP-positive neurons in the PFC of adult *Dcc*$^{lox/lox}$ mice that received bilateral microinfusions of the AAV-CaMKIIα-CreGFP vector. Scale bar= 20µm.

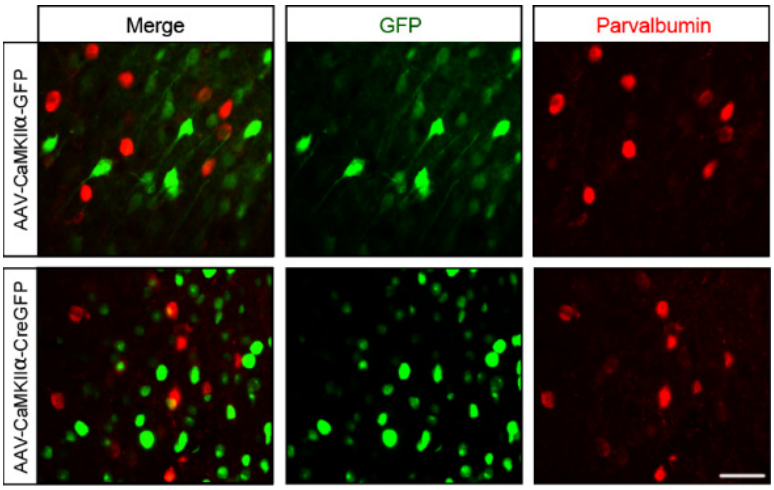

Figure S6. There is no GPF expression in parvalbumin-positive GABA neurons in the pregenual medial PFC of *Dcc*$^{lox/lox}$ mice injected with either AAV-CaMKIIα-CreGFP or control AAV-CaMKIIα-GFP, confirming that the expression of the viral construct is specificity to pyramidal neurons. Scale bar= 50µm.

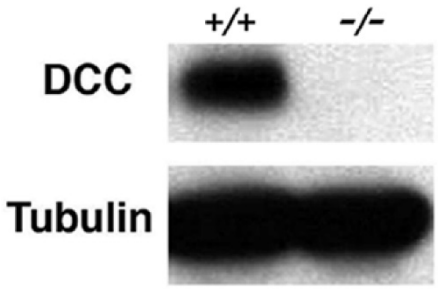

Figure S7. Confirmation of the specificity of the DCC antibody used in this study. The DCC antibody detects a single ~185 kDa band corresponding to DCC in wild-type (+/+) E17 mouse brain, but not in *Dcc* −/− E17 mouse brain. Adapted from (9).

Supplemental References

1. Krimpenfort P, Song, J-Y, Proost, N, Zevenhoven, J, Jonkers, J, & Berns, A (2012): Deleted in colorectal carcinoma suppresses metastasis in p53-deficient mammary tumours. *Nature* 482: 538-541.
2. Manitt C, Eng, C, Pokinko, M, Ryan, RT, Torres-Berrio, A, Lopez, JP, Yogendran, SV*, et al.* (2013): dcc orchestrates the development of the prefrontal cortex during adolescence and is altered in psychiatric patients. *Transl. Psychiatry* 3: e338.
3. Krishnan V, Han, M-H, Graham, DL, Berton, O, Renthal, W, Russo, SJ, LaPlant, Q*, et al.* (2007): Molecular Adaptations Underlying Susceptibility and Resistance to Social Defeat in Brain Reward Regions. *Cell* 131: 391-404.
4. Golden SA, Covington, HE, Berton, O, & Russo, SJ (2011): A standardized protocol for repeated social defeat stress in mice. *Nat. Protocols* 6: 1183-1191.
5. Rocchetti J, Isingrini, E, Dal Bo, G, Sagheby, S, Menegaux, A, Tronche, F, Levesque, D*, et al.* (2015): Presynaptic D2 Dopamine Receptors Control Long-Term Depression Expression and Memory Processes in the Temporal Hippocampus. *Biol Psychiatry* 77: 513-525.
6. Paxinos G & Franklin, K (2013): *Paxinos and Franklin's the Mouse Brain in Stereotaxic Coordinates,* Boston, Amsterdam: Elsevier/Academic Press
7. Grant A, Hoops, D, Labelle-Dumais, C, Prévost, M, Rajabi, H, Kolb, B, Stewart, J*, et al.* (2007): Netrin-1 receptor-deficient mice show enhanced mesocortical dopamine transmission and blunted behavioural responses to amphetamine. *Eur. J. Neurosci* 26: 3215-3228.
8. Flores C, Bhardwaj, SK, Labelle-Dumais, C, & Srivastava, LK (2009): Altered netrin-1 receptor expression in dopamine terminal regions following neonatal ventral hippocampal lesions in the rat. *Synapse* 63: 54-60.
9. Manitt C, Labelle-Dumais, C, Eng, C, Grant, A, Mimee, A, Stroh, T, & Flores, C (2010): Peri-Pubertal Emergence of UNC-5 Homologue Expression by Dopamine Neurons in Rodents. *PLoS ONE* 5: e11463.
10. Seaman C, Anderson, R, Emery, B, & Cooper, HM (2001): Localization of the netrin guidance receptor, DCC, in the developing peripheral and enteric nervous systems. *Mech. Dev* 103: 173-175.
11. Dweep H, Sticht, C, Pandey, P, & Gretz, N (2011): miRWalk – Database: Prediction of possible miRNA binding sites by “walking” the genes of three genomes. *J. Biomed. Inform* 44: 839-847.
12. Betel D, Wilson, M, Gabow, A, Marks, DS, & Sander, C (2008): The microRNA.org resource: targets and expression. *Nucl. Acids Res* 36: D149-D153.
13. Wang X (2008): miRDB: A microRNA target prediction and functional annotation database with a wiki interface. *RNA* 14: 1012-1017.
14. Maragkakis M, Reczko, M, Simossis, VA, Alexiou, P, Papadopoulos, GL, Dalamagas, T, Giannopoulos, G*, et al.* (2009): DIANA-microT web server: elucidating microRNA functions through target prediction. *Nucl. Acids Res* 37: W273-W276.
15. Lewis BP, Shih, Ih, Jones-Rhoades, MW, Bartel, DP, & Burge, CB (2003): Prediction of Mammalian MicroRNA Targets. *Cell* 115: 787-798.

16. Betel D, Koppal, A, Agius, P, Sander, C, & Leslie , C (2010): Comprehensive modeling of microRNA targets predicts functional non-conserved and non-canonical sites. *Genome Biol* 11: R90.

17. Mai J, Paxinos, G, & Voss, T (2007): *Atlas of the Human Brain,* San Diego: Elsevier/Academic Press

18. Small EM & Olson, EN (2011): Pervasive roles of microRNAs in cardiovascular biology. *Nature* 469: 336-342.